7.6.1 Appendix 7.A: The Okumura–Hata Model

Two forms of the Okumura-Hata model are available. In the first form, the pathloss (in dB) is written as

$$PL = PL_{\text{freespace}} + A_{\text{exc}} + H_{\text{cb}} + H_{\text{cm}} \tag{7.13}$$

where $PL_{\text{freespace}}$ is the freespace pathloss, A_{exc} is the excess pathloss (as a function of distance and frequency) for a BS height $h_{\text{b}} = 200$ m, and a MS height $h_{\text{m}} = 3$ m; it is shown in Fig. 7.12. The correction factors H_{cb} and H_{cm} are shown in Figs. 7.13 and 7.14, respectively.

The more common form is a curve fitting of Okumura's original results.[5] In that implementation, the pathloss is written as

$$PL = A + B\log(d) + C$$

where A, B, and C are factors that depend on frequency and antenna height.

$$A = 69.55 + 26.16\log(f_{\text{c}}) - 13.82\log(h_{\text{b}}) - a(h_{\text{m}}) \tag{7.14}$$

$$B = 44.9 - 6.55\log(h_{\text{b}}) \tag{7.15}$$

where f_{c} is given in MHz and d in km.

The function $a(h_{\text{m}})$ and the factor C depend on the environment:

- small and medium-size cities:

$$a(h_{\text{m}}) = (1.1\log(f_{\text{c}}) - 0.7)h_{\text{m}} - (1.56\log(f_{\text{c}}) - 0.8) \tag{7.16}$$

$$C = 0\ . \tag{7.17}$$

- metropolitan areas

$$a(h_{\text{m}}) = \begin{cases} 8.29(\log(1.54h_{\text{m}})^2 - 1.1 & \text{for } f \leq 200 \text{ MHz} \\ 3.2(\log(11.75h_{\text{m}})^2 - 4.97 & \text{for } f \geq 400 \text{ MHz} \end{cases} \tag{7.18}$$

$$C = 0\ . \tag{7.19}$$

- suburban environments

$$C = -2[\log(f_{\text{c}}/28)]^2 - 5.4\ . \tag{7.20}$$

- rural area

$$C = -4.78[\log(f_{\text{c}})]^2 + 18.33\log(f_{\text{c}}) - 40.98\ . \tag{7.21}$$

The function $a(h_{\text{m}})$ in suburban and rural areas is the same as for urban (small and medium-sized cities) areas.

[5] Note that the results from the curve fitting can be slighltly different from the results of Eq. (7.13).

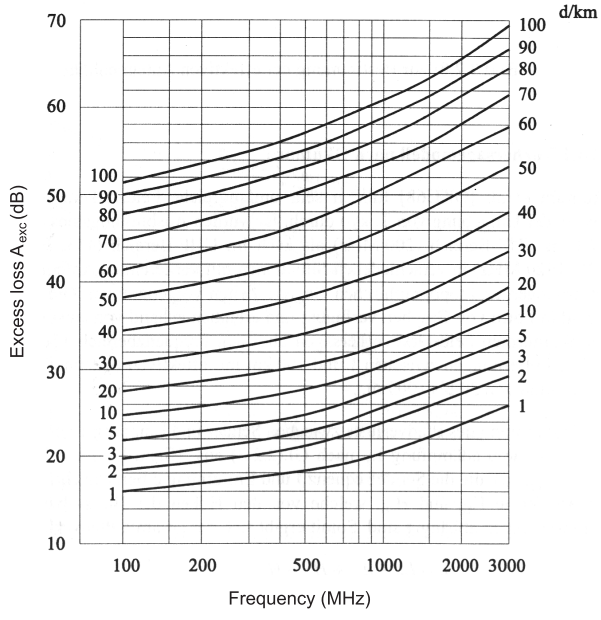

Figure 7.12 Pathloss according to the Okumura-Hata model. Excess loss is the difference between Okumura-Hata pathloss (at the reference points $h_b = 200m$, $h_m = 3m$), and free space loss.
Reproduced from Okumura et al. [1968].

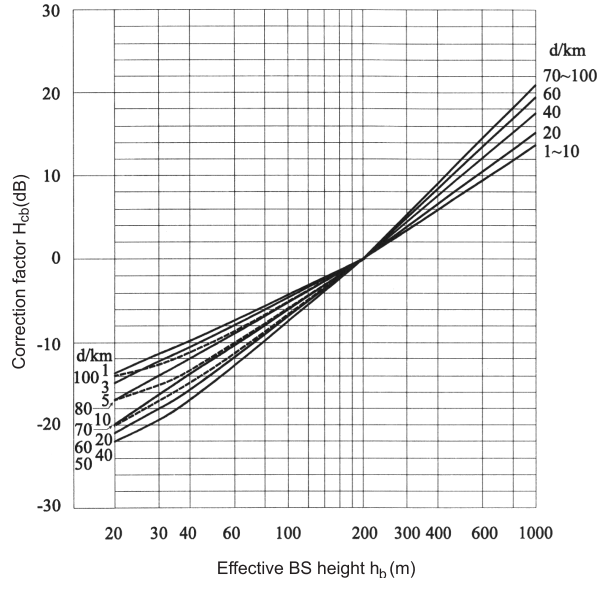

Figure 7.13 Correction factor for base station height.
Reproduced from Okumura et al. [1968].

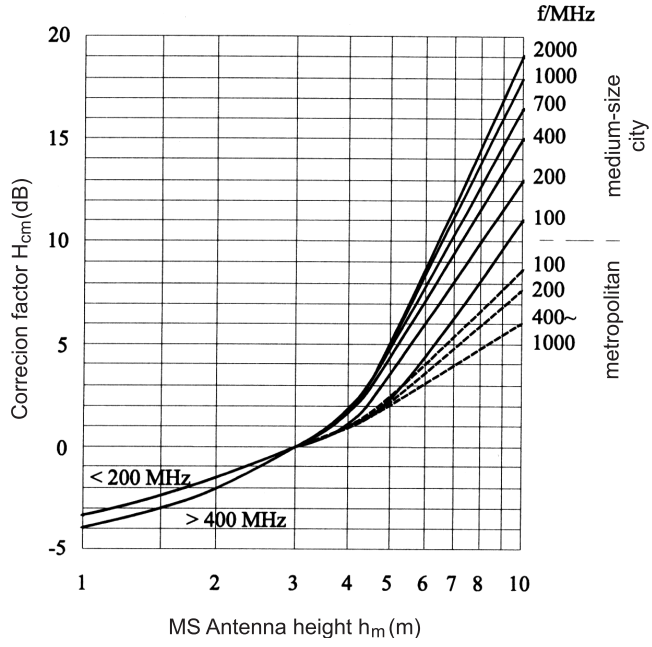

Figure 7.14 Correction factor for mobile station height.
Reproduced from Okumura et al. [1968].

Table 7.1 Range of validity for the Okumura-Hata model.

carrier frequency	f_c	150...1500 MHz
effective BS-antenna height	h_b	30...200 m
effective MS-antenna height	h_m	1...10 m
distance	d	1...20 km

Table 7.1 gives the parameter range in which the model is valid. It is noteworthy that the parameter range does not encompass the 1800 MHz frequency range most commonly used for second-and third generation cellular systems. This problem was solved by the COST 231 - Hata model, which extends the validity region to the 1500 - 2000 MHz range by defining

$$\begin{aligned} A &= 46.3 + 33.9\log(f_c) - 13.82\log(h_b) - a(h_m) \\ B &= 44.9 - 6.55\log(h_b) \end{aligned} \tag{7.22}$$

where $a(h_m)$ is defined in Eq. (7.16). C is 0 in small and medium-sized cities, and 3 in metropolitan areas.

The Okumura-Hata model also assumes that there are no dominant obstacles between the BS and the MS, and that the terrain profile changes only slowly. [Badsberg et al. 1995] and [Isidoro et al. 1995] suggested correction factors that are intended to avoid these restrictions; however, they have not found the widespread acceptance of the COST 231 correction factors.

7.6.2 Appendix 7.B: The COST 231–Walfish–Ikegami Model

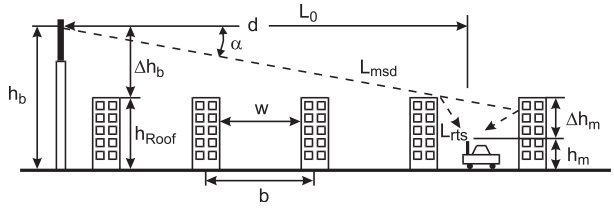

Figure 7.15 Parameters in the COST 231-Walfish-Ikegami model.
Reproduced with permission from Damosso and Correia [1999] © European Union.

The COST 231 model is a pathloss model for the case of small distances between MS and BS, and/or small height of the MS. The total pathloss for the LOS case is given by

$$PL = 42.6 + 26\log(d) + 20\log(f_c) \tag{7.23}$$

for $d \geq 20$ m, where again d is in units of kilometers, and f_c is in units of MHz.

For the NLOS case, the pathloss consists of the free-space pathloss L_0, the *multiscreen loss* L_{msd} along the propagation path, and the attenuation from the last roofedge to the MS, L_{rts} (*roof-top-to-street diffraction and scatter loss*):

$$PL = \begin{cases} PL_0 + L_{rts} + L_{msd} & \text{for } L_{rts} + L_{msd} > 0 \\ PL_0 & \text{for } L_{rts} + L_{msd} \leq 0 \end{cases} . \tag{7.24}$$

The free-space pathloss is

$$L_0 = 32.4 + 20\log d + 20\log f_c \ . \tag{7.25}$$

Ikegami derived the diffraction loss L_{rts} as

$$L_{rts} = -16.9 - 10\log w + 10\log f_c + 20\log \Delta h_m + L_{ori} \tag{7.26}$$

where w is the width of the street in meters, and

$$\Delta h_m = h_{Roof} - h_m \tag{7.27}$$

is the difference between the building height h_{Roof} and the height of the MS h_m. The orientation of the street is taken into account by an empirical correction factor L_{ori}

$$L_{ori} = \begin{cases} -10 + 0.354\varphi & \text{for } 0^\circ \leq \varphi \leq 35^\circ \\ 2.5 + 0.075(\varphi - 35) & \text{for } 35^\circ \leq \varphi \leq 55^\circ \\ 4.0 - 0.114(\varphi - 55) & \text{for } 55^\circ \leq \varphi \leq 90^\circ \end{cases} \tag{7.28}$$

where φ is the angle between the street orientation and the direction of incidence in degrees.

For the computation of the multiscreen loss L_{msd}, building edges are modeled as screens. The multiscreen loss is then given as [Walfish and Bertoni 1988]:

$$L_{msd} = L_{bsh} + k_a + k_d \log d + k_f \log f_c - 9\log b \tag{7.29}$$

where b is the distance between two buildings (in meters). Furthermore,

$$L_{\mathrm{bsh}} = \begin{cases} -18\log(1+\Delta h_{\mathrm{b}}) & \text{for } h_{\mathrm{b}} > h_{\mathrm{Roof}} \\ 0 & \text{for } h_{\mathrm{b}} \le h_{\mathrm{Roof}} \end{cases} \tag{7.30}$$

$$k_{\mathrm{a}} = \begin{cases} 54 & \text{for } h_{\mathrm{b}} > h_{\mathrm{Roof}} \\ 54 - 0.8\Delta h_{\mathrm{b}} & \text{for } d \ge 0.5 \text{ km and } h_{\mathrm{b}} \le h_{\mathrm{Roof}} \\ 54 - 0.8\Delta h_{\mathrm{b}}\dfrac{d}{0.5} & \text{for } d < 0.5 \text{ km and } h_{\mathrm{b}} \le h_{\mathrm{Roof}} \end{cases} \tag{7.31}$$

where

$$\Delta h_{\mathrm{b}} = h_{\mathrm{b}} - h_{\mathrm{Roof}} \tag{7.32}$$

and h_{b} is the height of the BS. The dependence of the pathloss on the frequency and distance is given via the parameters k_{d} and k_{f} in Eq. (7.29):

$$k_{\mathrm{d}} = \begin{cases} 18 & \text{for } h_{\mathrm{b}} > h_{\mathrm{Roof}} \\ 18 - 15\dfrac{\Delta h_{\mathrm{b}}}{h_{\mathrm{Roof}}} & \text{for } h_{\mathrm{b}} \le h_{\mathrm{Roof}} \end{cases} \tag{7.33}$$

$$k_{\mathrm{f}} = -4 + \begin{cases} 0.7\left(\dfrac{f_{\mathrm{c}}}{925} - 1\right) & \text{for medium-size cities} \\ & \text{suburban areas with average vegetation density} \\ 1.5\left(\dfrac{f_c}{925} - 1\right) & \text{for metropolitan areas} \end{cases} . \tag{7.34}$$

Table 7.2 gives the validity range for this model

Further assumptions include a Manhatten grid (streets intersecting at right angles), constant building height, and flat terrain. Furthermore, the model does not include the effect of waveguiding through street canyons, which can lead to an underestimation of the received fieldstrength.

Table 7.2 Range of validity for the COST 231-Walfish-Ikegami model.

carrier frequency	f_{c}	800...2000 MHz
height of the BS antenna	h_{b}	4...50 m
height of the MS antenna	h_{m}	1...3 m
distance	d	0.02...5 km

7.6.3 Appendix 7.C: The COST 207 GSM Model

The COST 207 model [Failii 1989] gives normalized scattering functions, as well as amplitude statistics, for four classes of environments: Rural Area, Typical Urban, Bad Urban, and Hilly Terrain. The following PDPs are used:

- Rural Area (RA)

$$P_h(\tau) = \begin{cases} \exp\left(-9.2\dfrac{\tau}{\mu s}\right) & \text{for } 0 < \tau < 0.7\mu s \\ 0 & \text{elsewhere} \end{cases} . \tag{7.35}$$

- Typical Urban area (TU)

$$P_h(\tau) = \begin{cases} \exp\left(-\dfrac{\tau}{\mu s}\right) & \text{for } 0 < \tau < 7\mu s \\ 0 & \text{elsewhere} \end{cases} . \tag{7.36}$$

- Bad Urban area (BU)

$$P_h(\tau) = \begin{cases} \exp\left(-\dfrac{\tau}{\mu s}\right) & \text{for } 0 < \tau < 5\mu s \\ 0.5\exp\left(5 - \dfrac{\tau}{\mu s}\right) & \text{for } 5 < \tau < 10\mu s \\ 0 & \text{elsewhere} \end{cases} . \tag{7.37}$$

- Hilly Terrain (HT)

$$P_h(\tau) = \begin{cases} \exp\left(-3.5\dfrac{\tau}{\mu s}\right) & \text{for } 0 < \tau < 2\mu s \\ 0.1\exp\left(15 - \dfrac{\tau}{\mu s}\right) & \text{for } 15 < \tau < 20\mu s \\ 0 & \text{elsewhere} \end{cases} . \tag{7.38}$$

In a tapped delay-line realization, each channel has a Doppler spectrum $P_s(\nu, \tau_i)$, where i is the index of the tap. The following four types of Doppler spectra are defined in the COST 207 model, where $\nu_{\max}$ represents the maximum Doppler shift and $G(A, \nu_1, \nu_2)$ is the Gaussian function

$$G(A, \nu_1, \nu_2) = A\exp\left(-\frac{(\nu - \nu_1)^2}{2\nu_2^2}\right) \tag{7.39}$$

and A is a normalization constant chosen so that $\int P_s(\nu, \tau_i)d\nu = 1$.

a) *CLASS* is the classical (Jakes) Doppler spectrum and is used for paths with delays not in excess of 500 ns ($\tau_i \leq 0.5\ \mu s$):

$$P_s(\nu, \tau_i) = \frac{A}{\sqrt{1 - \left(\dfrac{\nu}{\nu_{\max}}\right)^2}} \tag{7.40}$$

for $\nu \in [-\nu_{\max}, \nu_{\max}]$;

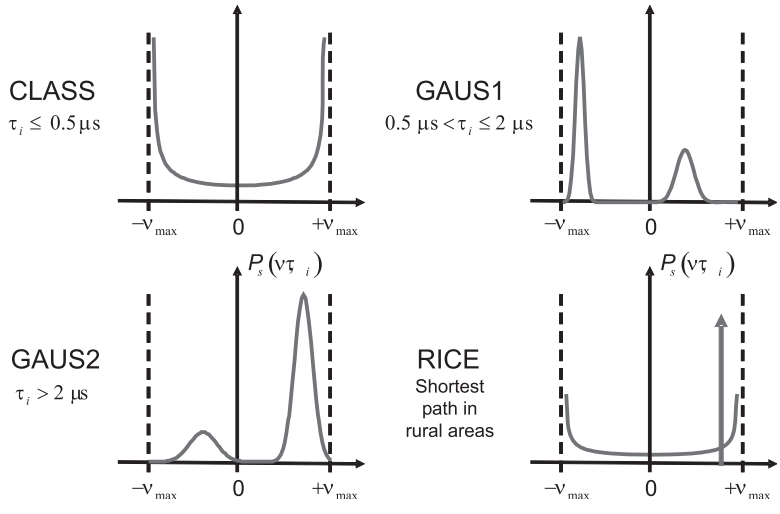

Figure 7.16 Doppler spectra used in GSM channel models.

b) *GAUS1* is the sum of two Gaussian functions and is used for excess delay times in the range of 500 ns to 2 μs (0.5 $\mu s \leq \tau_i \leq 2$ μs):

$$P_s(\nu, \tau_i) = G(A, -0.8\nu_{\max}, 0.05\nu_{\max}) + G(A_1, 0.4\nu_{\max}, 0.1\nu_{\max}) \tag{7.41}$$

where A_1 is 10 dB smaller than A;

c) *GAUS2* is also the sum of two Gaussian functions and is used for paths with delays in excess of 2 μs ($\tau_i \geq 2$ μs):

$$P_s(\nu, \tau_i) = G(B, 0.7\nu_{\max}, 0.1\nu_{\max}) + G(B_1, -0.4\nu_{\max}, 0.15\nu_{\max}) \tag{7.42}$$

where B_1 is 15 dB smaller than B;

d) *RICE* is the sum of a classical Doppler spectrum and one direct path, such that the total multipath contribution is equal to that of the direct path. This spectrum is used for the shortest path of the model for propagation in rural areas:

$$P_s(\nu, \tau_i) = \frac{0.41}{2\pi\nu_{\max}\sqrt{1 - \left(\dfrac{\nu}{\nu_{\max}}\right)^2}} + 0.91\delta(\nu - 0.7\nu_{\max}) \tag{7.43}$$

for $\nu \in [-\nu_{\max}, \nu_{\max}]$;

Table 7.3 Parameters for rural (non-hilly) area (RA)

Tap#	Delay [μs]	Power [dB]	Doppler category
1	0	0	RICE
2	0.2	-2	CLASS
3	0.4	-10	CLASS
4	0.6	-20	CLASS

Table 7.4 Parameters for urban (non-hilly) area (TU)

Tap#	Delay [μs]	Power [dB]	Doppler category
1	0	-3	CLASS
2	0.2	0	CLASS
3	0.6	-2	GAUS1
4	1.6	-6	GAUS1
5	2.4	-8	GAUS2
6	5.0	-10	GAUS2

Table 7.5 Parameters for hilly urban area (BU)

Tap#	Delay [μs]	Power [dB]	Doppler category
1	0	-3	CLASS
2	0.4	0	CLASS
3	1.0	-3	GAUS1
4	1.6	-5	GAUS1
5	5.0	-2	GAUS2
6	6.6	-4	GAUS2

Table 7.6 Parameters for hilly terrain (HT)

Tap#	Delay [μs]	Power [dB]	Doppler category
1	0	0	CLASS
2	0.2	-2	CLASS
3	0.4	-4	CLASS
4	0.6	-7	CLASS
5	15	-6	GAUS2
6	17.2	-12	GAUS2

7.6.4 Appendix 7.D: The ITU-R Models

For the selection of the air interface of third-generation cellular systems, the *International Telecommunications Union (ITU)* developed another set of models that is available only as a tapped-delay-line implementation [ITU 1997]. It specifies three environments: indoor, pedestrian (including outdoor to indoor), and vehicular (with high BS antennas). For each of those environments, two channels are defined: channel A (low delay spread case) and channel B (high delay spread). The occurrence rate of these two models is also specified; all those parameters are given in Table 7.7. The amplitudes follow a Rayleigh distribution; the Doppler spectrum is uniform between $-\nu_{max}$ and ν_{max} for the indoor case and is a classical Jakes spectrum for the pedestrian and vehicular environments.

In contrast to the COST207 model, the ITU model also specifies the pathloss (in dB) depending on the distance d:

- *indoor*:

$$PL = 37 + 30\log_{10} d + 18.3 \cdot N_{\text{floor}}^{\left(\frac{N_{\text{floor}}+2}{N_{\text{floor}}+1} - 0.46\right)} . \tag{7.44}$$

- *pedestrian*:

$$PL = 40\log_{10} d + 30\log_{10} f_c + 49 \tag{7.45}$$

where again d is in km and f_c is in MHz. For the outdoor-to-indoor case, the additional building penetration loss (in dB) is modeled as a normal variable with 12 dB mean and 8 dB standard deviation

Table 7.7 Tapped-delay-line implementation of ITU-R models.

Tap No.	delay/ns	power/dB	delay/ns	power/dB
INDOOR	**CHANNEL A** (50%)		**CHANNEL B** (45%)	
1	0	0	0	0
2	50	-3	100	-3.6
3	110	-10	200	-7.2
4	170	-18	300	-10.8
5	290	-26	500	-18.0
6	310	-32	700	-25.2
PEDESTRIAN	**CHANNEL A** (40%)		**CHANNEL B** (55%)	
1	0	0	0	0
2	110	-9.7	200	-0.9
3	190	-19.2	800	-4.9
4	410	-22.8	1200	-8.0
5			2300	-7.8
6			3700	-23.9
VEHICULAR	**CHANNEL A** (40%)		**CHANNEL B** (55%)	
1	0	0	0	-2.5
2	310	-1	300	0
3	710	-9	8900	-12.8
4	1090	-10	12900	-10.0
5	1730	-15	17100	-25.2
6	2510	-20	20000	-16.0

- *vehicular*:

$$PL = 40(1 - 4 \cdot 10^{-3} \Delta h_{\mathrm{b}}) \log_{10} d - 18 \log_{10} \Delta h_{\mathrm{b}} + 21 \log_{10} f_{\mathrm{c}} + 80 \tag{7.46}$$

  where Δh_{b} is the BS height measured from the rooftop level; the model is valid for $0 < \Delta h_b < 50$ m.

In all three cases, lognormal shadowing is imposed. The standard deviation is 12 dB for the indoor case, and 10 dB in the vehicular and outdoor pedestrian case. The autocorrelation function of the shadowing is assumed to be exponential, $ACF(\Delta x) = \exp(-\ln(2)|\Delta x|/d_{\mathrm{corr}})$ where the correlation length d_{corr} is 20 m in vehicular environments, but not specified for other environments.

The ITU models have been widely used, because they were accepted by international standards organizations. However, they are not very satisfactory from a scientific point of view. It is difficult to motivate differences in the power delay profile of pedestrian and vehicular channels, while neglecting the differences between suburban and metropolitan areas. Also, some of the channels have regularly spaced taps, which leads to a periodicity in frequency of the transfer function; this can lead to problems when evaluting the correlation between duplex frequencies (see Chapter 17). Finally, the number of taps is too low for realistic modeling of 5 MHz wide systems.

7.6.5 Appendix 7.E: The 3GPP Spatial Channel Model

The 3GPP and 3GPP2 industry alliances jointly developed channel models that are to be used for the evaluation of cellular systems with multiple antenna elements. The bandwidth of the tested systems should not exceed 5 MHz. The models are defined for three environments, namely urban microcells, urban macrocells, and suburban macrocells. The model is a mixed geometrical–stochastic model that can simulate a cellular layout including interference. The description closely follows [Calcev et al. 2007].

Pathloss

In a first step, the environment and the locations of N_{BS} BSs are chosen, and locations of the MSs are generated at random. One also needs to specify other user-specific quantities, such as their velocity vector $\mathbf{v}$, with its direction θ_v drawn from a uniform $[0, 360^\circ)$ distribution, as well as the specifics of the MS antenna or antenna array such as array orientation, Ω_{MS}, etc. Figure 7.17 illustrates the various angle definitions.

For the suburban and urban macrocells, the pathloss is determined as:

$$\begin{aligned} PL[dB] = {} & (44.9 - 6.55\log_{10}(h_{BS}))\log_{10}\left(\frac{d}{1000}\right) \\ & + 45.5 + (35.46 - 1.1h_{MS})\log_{10}(f_c) \\ & - 13.82\log_{10}(h_{MS}) + 0.7h_{MS} + C \end{aligned} \tag{7.47}$$

where h_{BS} is the BS antenna height in meters, h_{MS} the MS antenna height in meters, f_c the carrier frequency in MHz, d is the distance between the BS and MS in meters (has to be at least 35 m), and C is a constant factor ($C = 0$ dB for suburban macro and $C = 3$ dB for urban macro). The microcell non-line-of-sight (NLOS) pathloss is:

$$PL[dB] = -55.9 + 38\log_{10}(d) + (24.5 + \frac{f_c}{616.67})\log_{10}(f_c) \tag{7.48}$$

Narrowband Parameters

The delay-spread $\sigma_{DS,n}$, BS angle-spread $\sigma_{AS,n}$ and shadow fading $\sigma_{SF,n}$ parameters of the signal from BS n, where $n = 1, \ldots, N_{BS}$, to a given user can be written as:

$$10\log_{10}(\sigma_{DS,n}) = \mu_{DS} + \in_{DS} X_{1n} \tag{7.49}$$

$$10\log_{10}(\sigma_{AS,n}) = \mu_{AS} + \in_{AS} X_{2n} \tag{7.50}$$

$$10\log_{10}(\sigma_{SF,n}) = \in_{SF} X_{3n} \tag{7.51}$$

In the above equations X_{1n}, X_{2n}, X_{3n} are zero-mean, unit-variance Gaussian random variables. μ_{DS} and μ_{AS} represent the median of the delay-spread and angle-spreads in dB. Similarly, the $\in$-coefficients are the log-normal variances of each parameter. The values of μ and ε are given in

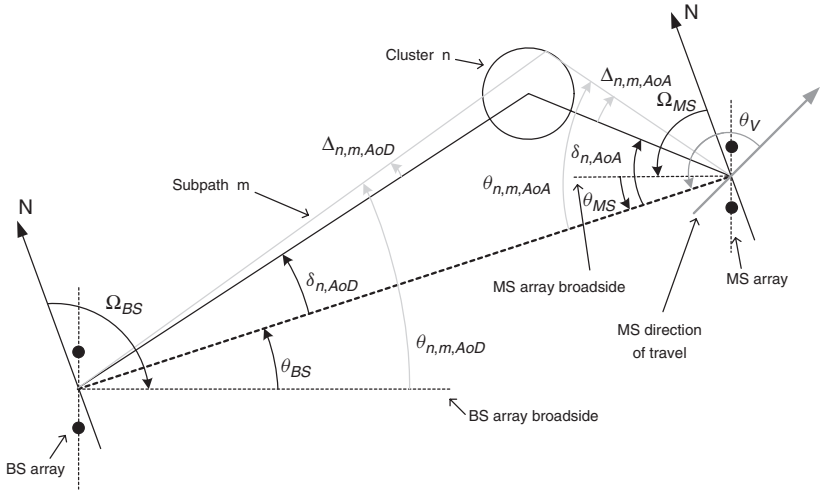

Figure 7.17 Angular variables definitions. From [Calcev et al. 2007] © IEEE.

Table 7.8. Once $\sigma_{DS,n}$ and $\sigma_{AS,n}$ have been determined, they are used to generate the relative delays and mean angles of departure of the intra-cluster paths.

Correlations between shadowing, delay spread, and angular spread are expressed in terms of a covariance matrix **A**, as seen in Eq. (7.52), whose A_{ij} component represents the correlations between X_{in} and X_{jn}, with $i, j = 1, 2, 3$. Correlations between spreads from different BSs are expressed by a matrix **B** with B_{ij} representing the correlations between X_{in} and X_{jm}, for $i, j = 1, 2, 3$ and $n \neq m$.

$$\mathbf{A} = \begin{bmatrix} 1 & \rho_{DA} & \rho_{DF} \\ \rho_{DA} & 1 & \rho_{AF} \\ \rho_{DF} & \rho_{AF} & 1 \end{bmatrix} \qquad \mathbf{B} = \begin{bmatrix} 0 & 0 & 0 \\ 0 & 0 & 0 \\ 0 & 0 & \zeta \end{bmatrix} \tag{7.52}$$

where

$$\begin{aligned} \rho_{DA} &= E\left[X_{1n}X_{2n}\right] = +0.5 \\ \rho_{DF} &= E\left[X_{2n}X_{3n}\right] = -0.6 \\ \rho_{AF} &= E\left[X_{3n}X_{1n}\right] = -0.6 \\ \zeta &= E\left[X_{3n}X_{3m}\right] = +0.5 \quad n \neq m \end{aligned}$$

Wideband Parameters–Macrocellular Case

The wideband parameters are determined the following way:

1. **Path Delays**: The (random) delays of the paths are written as

$$\tau_n' = -r_{DS}\sigma_{DS} \ln z_n \quad n = 1, \ldots, N \tag{7.53}$$

Table 7.8 Environment Parameters

Channel Scenario	Suburban Macro	Urban Macro	Urban Micro
Number of paths	6	6	6
Number of sub-paths (M) per-path	20	20	20
Mean rms AS at BS	$E(\sigma_{AS}) = 5^\circ$	$E(\sigma_{AS}) = 8^\circ, 15^\circ$	NLOS: $E(\sigma_{AS}) = 19^\circ$
AS at BS as a lognormal RV	$\mu_{AS} = 0.69$	8° $\mu_{AS} = 0.810$	N/A
$\sigma_{AS} = 10^{(\varepsilon_{AS} \cdot x + \mu_{AS})}$	$\varepsilon_{AS} = 0.13$	$\varepsilon_{AS} = 0.34$	
$x \sim N(0, 1)$		15° $\mu_{AS} = 1.18$	
σ_{AS} in degrees		$\varepsilon_{AS} = 0.210$	
$r_{AS} = \sigma_{AoD}/\sigma_{AS}$	1.2	1.3	N/A
Per-path AS at BS (Fixed)	2°	2°	5° (LOS and NLOS)
BS per-path AoD Distribution	$N(0, \sigma^2_{AoD})$ where	$N(0, \sigma^2_{AoD})$ where	$U(-40^\circ, 40^\circ)$
standard deviation	$\sigma_{AoD} = r_{AS} \cdot \sigma_{AS}$	$\sigma_{AoD} = r_{AS} \cdot \sigma_{AS}$	
Mean rms AS at MS	$E(\sigma_{AS,MS}) = 68^\circ$	$E(\sigma_{AS,MS}) = 68^\circ$	$E(\sigma_{AS,MS}) = 68^\circ$
Per-path AS at MS (Fixed)	35°	35°	35°
MS Per-path AoA Distribution	$N(0, \sigma^2_{AoA}(Pr))$	$N(0, \sigma^2_{AoA}(Pr))$	$N(0, \sigma^2_{AoA}(Pr))$
Delay spread as a lognormal RV	$\mu_{DS} = -6.80$	$\mu_{DS} = -6.18$	N/A
$\sigma_{DS} = 10^{(\varepsilon_{DS} \cdot x + \mu_{DS})}$	$\varepsilon_{DS} = 0.288$	$\varepsilon_{DS} = 0.18$	
$x \sim N(0, 1)$			
σ_{DS} in μsec			
Mean total rms Delay Spread	$E(\sigma_{DS}) = 0.17\mu s$	$E(\sigma_{DS}) = 0.65\mu s$	$E(\sigma_{DS}) = 0.251\mu s$ (output)
$r_{DS} = \sigma_{delays}/\sigma_{DS}$	1.4	1.7	N/A
Distribution for path delays			$U(0, 1.2\mu s)$
Lognormal shadowing	8 dB	8 dB	NLOS: 10 dB
standard deviation σ_{SF}			LOS: 4 dB
Pathloss model (dB)	$31.5 + 35\log_{10}(d)$	$34.5 + 35\log_{10}(d)$	NLOS: $34.53 + 38\log_{10}(d)$
d is in meters			LOS: $30.18 + 26\log_{10}(d)$

where z_n $(n = 1, \ldots, N)$ are i.i.d. random variables with uniform distribution $U(0, 1)$. The τ'_n variables are then ordered so that $\tau'_{(N)} > \tau'_{(N-1)} > \cdots > \tau'_{(1)}$. Then their minimum is subtracted from all, i.e., $\tau_n = \left(\tau'_{(n)} - \tau'_{(1)}\right)$, with $n = 1, \ldots, N$, so that $\tau_N > \cdots > \tau_1 = 0$.

2. **Path Powers**: the average powers of the N paths are expressed as

$$P'_n = e^{\frac{(1-r_{DS})\tau_n}{r_{DS} \cdot \sigma_{DS}}} \cdot 10^{-0.1\xi_n} \qquad n = 1, \ldots, N. \tag{7.54}$$

ξ_n for $n = 1, \ldots, N$ are i.i.d. Gaussian random variables with standard deviation $\sigma_{RND} = 3$dB, signifying the fluctuations of the powers away from the average exponential behavior. Average powers are then normalized, so that the total average power for all N paths is equal to unity.

3. **Angles of Departure (AoD)**: the distribution of angles of departure at the BS has a Gaussian distribution with variance $\sigma_{AoD} = r_{AS}\sigma_{AS}$. The values of the AoD are thus initially given by

$$\delta'_n \sim N(0, \sigma^2_{AoD}), \tag{7.55}$$

where $n = 1, \ldots, N$. These variables are given in degrees and they are ordered in increasing absolute value so that $\left|\delta'_{(1)}\right| < \left|\delta'_{(2)}\right| < \cdots < \left|\delta'_{(N)}\right|$. The AoDs $\delta_{n,AoD}$, $n = 1, \ldots, N$ are assigned to the ordered variables so that $\delta_{n,AoD} = \delta'_{(n)}$, $n = 1, \ldots, N$.

4. **Angles of Arrival (AoA)**: The AoA at the MS has a truncated normal distribution with mean zero with respect to the LOS direction, i.e.

$$\delta_{n,AoA} \sim N(0, \sigma^2_{n,AoA}), \tag{7.56}$$

with $n = 1, \ldots, N$. The variance of each path $\sigma_{n,AoA}$ depends on the relative power of that path:

$$\sigma_{n,AoA} = 104.12^\circ \cdot (1 - \exp(0.2175 \cdot P_{n,dBr})). \tag{7.57}$$

The $\sigma_{n,AoA}$ represents the standard deviation of the non-circular angle spread and $P_{n,dBr} < 0$ is the relative power of the $n\text{-}th$ path, in dBr, with respect to total received power.

Wideband Parameters–Microcellular Case

1. **Path Delays**: The delays τ_n, $n = 1, \ldots, N$ are i.i.d. random variables drawn from a uniform distribution $U(0, 1.2\mu sec)$. The minimum of these delays is subtracted from all so that the first delay is zero.
2. **Path Powers**: The power of each of the N paths depends on the delay as

$$P'_n = 10^{-(\tau_n + 0.1 z_n)} \tag{7.58}$$

where τ_n are the delays of each path in units of microseconds, and z_n ($n = 1, \ldots, N$) are i.i.d. zero mean Gaussian random variables with a standard deviation of 3dB. Average powers are normalized so that total average power for all N paths is equal to unity.

3. **Angles of Departure (AoD)**: In the microcell case the AoD of each of the N paths at the base can be modelled as i.i.d. uniformly distributed random variables between -40 and $+40$ degrees:

$$\delta_{n,AoD} \sim U(-40^\circ, +40^\circ), \tag{7.59}$$

where $n = 1, \ldots, N$. One can now associate a power to each of the path delays determined above. Note that, unlike the macrocell environment, the AoDs do not need to be sorted before being assigned to a path power.

4. **Angles of Arrival (AoA)**: The mean AoA of each path can be determined similar to the way discussed in the macrocell case, i.e., i.i.d Gaussian random variables

$$\delta_{n,AoA} \sim N(0, \sigma^2_{n,AoA}), \quad \text{where } n = 1, \ldots, N \tag{7.60}$$

$$\sigma_{n,AoA} = 104.12^\circ \left[1 - \exp(0.265 \cdot P_{dBr})\right] \tag{7.61}$$

where P_{dBr} is the relative power of the $n\text{-}th$ path in dBr. When the LOS model is used, the AoA for the direct component is set equal to the LOS path direction.

Generation of Fast-Fading Coefficients

We now describe how to generate fast fading coefficients for wideband time-varying MIMO channels with N_t transmit antennas and N_r receive antennas. The fast-fading coefficients for each of the N paths are constructed by the superposition of M individual sub-paths. The m-th component ($m = 1, \ldots, M$) is characterized by a relative angular offset to the mean AoD of the path at the BS, a relative angular offset to the mean AoA at the MS, a power and an overall phase. M is fixed to $M = 20$, and all sub-paths have the same power P_n/M. The sub-path delays are identical and equal to their corresponding path's delay. The overall phase of each subpath $\Phi_{n,m}$ is i.i.d., with a uniform distribution between 0 and 2π. The relative offset of the $m\text{-}th$ subpath $\Delta_{n,m,AoD}$ at the BS, and $\Delta_{n,m,AoA}$ at the MS are given in Table 7.9. These offsets are chosen to result to the desired fixed per-path angle spreads (2° for the macrocell environments, 5° for the microcell environment for $\Delta_{n,m,AoD}$ at the BS and 35° at the MS for $\Delta_{n,m,AoA}$). These per-path angle spreads are different from the narrowband angle spread σ_{AS} of the composite signal with N paths.

Table 7.9 Sub-path AoD and AoA offsets

Sub-path number (m)	Offset at BS, AS = 2°, Macrocell $\Delta_{n,m,AoD}$ (degrees)	Offset at BS AS = 5° Microcell $\Delta_{n,m,AoD}$ (degrees)	Offset at MS AS = 35° $\Delta_{n,m,AoA}$ (degrees)
1, 2	±0.0894	±0.2236	±1.5649
3, 4	±0.2826	±0.7064	±4.9447
5, 6	±0.4984	±1.2461	±8.7224
7, 8	±0.7431	±1.8578	±13.0045
9, 10	±1.0257	±2.5642	±17.9492
11, 12	±1.3594	±3.3986	±23.7899
13, 14	±1.7688	±4.4220	±30.9538
15, 16	±2.2961	±5.7403	±40.1824
17, 18	±3.0389	±7.5974	±53.1816
19, 20	±4.3101	±10.7753	±75.4274

The BS and MS sub-paths are associated by connecting their respective parameters. The *n-th* BS path (defined by its delay τ_n, power P_n, and AoD $\delta_{n,AoD}$) is uniquely associated with the *n-th* MS path (defined by its AoA $\delta_{n,AoA}$) because of the ordering. For the *n-th* path, each of the M BS sub-paths (defined by its offset $\Delta_{n,m,AoD}$) is randomly paired with a MS sub-path (defined by its offset $\Delta_{n,m,AoA}$) and the phases defined by $\Phi_{n,m}$ are applied. To simplify the notation, a renumbering of the M MS sub-path offsets with their newly associated BS sub-path is done. Summarizing, for the *n-th* path, the AoD of the *m-th* sub-path (from the BS broadside) is

$$\theta_{n,m,AoD} = \theta_{BS} + \delta_{n,AoD} + \Delta_{n,m,AoD}, \tag{7.62}$$

Similarly, the AoA of the *m-th* sub-path for the *n-th* path (from the MS array broadside) is

$$\theta_{n,m,AoA} = \theta_{MS} + \delta_{n,AoA} + \Delta_{n,m,AoA} \tag{7.63}$$

The antenna gains are dependent on these sub-path AoDs and AoAs. For the BS and MS, these are given respectively as $|G_{BS}(\theta_{n,m,AoD})|^2$ and $|G_{MS}(\theta_{n,m,AoA})|^2$, where $G(\theta)$ is the corresponding complex antenna response to and from radiation with angle θ.

Lastly, the path loss, based on the BS to MS distance and the log normal shadow fading, is applied to each of the sub-path powers of the channel model.

The channel transfer function between receiver u and transmitter s at path n and time t is

$$\begin{aligned} h_{u,s,n}(t) = \sqrt{\frac{P_n \sigma_{SF}}{M}} \sum_{m=1}^{M} \big(& e^{jk\|\mathbf{v}\| \cos(\theta_{n,m,AoA} - \theta_v)t} \\ & G_{BS}(\theta_{n,m,AoD}) \cdot e^{j(kd_s \sin(\theta_{n,m,AoD}) + \Phi_{n,m})} \\ & G_{MS}(\theta_{n,m,AoA}) \cdot e^{jkd_u \sin(\theta_{n,m,AoA})} \big) \end{aligned} \tag{7.64}$$

Further Options

In addition, the model also specifies several options including line-of-sight situations in urban microcells, waveguiding in street canyons, far scatterer clusters, and polarization diversity. Details can be found in Calcev et al. [2007].

7.6.6 Appendix 7.F: The ITU-Advanced Channel Model

The ITU has defined a set of channel models for the evaluation of IMT-Advanced systems proposals. The modeling method is almost identical to the 3GPP model; but for the convenience of the reader, we repeat here the step-by-step instructions for implementation (closely following the offical report [ITU 2008]). Also, the ITU models are based on more extensive measurement campaigns (mostly done within the framework of the EU projects WINNER and WINNER 2), and cover a larger range of scenarios.

The double-directional impulse response consists of a number of (delay) taps, where each tap consists of multiple rays that have different DOAs and DODs. The delays and angles all depend on large-scale parameters that can change from drop to drop.

The following steps have to be performed in order to get the channel in a particular environment:

1. The ITU models are based on the "drop" concept. Thus, in a first step, locations of the base stations are selected. For the mobile stations, we select locations, orientation, and velocity vectors, according to probability density functions.[6]
2. Assign whether an MS has LOS or NLOS, according to the pdf given in Table 7.10

Table 7.10 Probability for line-of-sight. For meaning of scenario abbreviations, see Table 7.11.

Scenario	LoS probability as a function of distance, d(m)
InH	$P_{LOS} = \begin{cases} 1, & d \le 18 \\ \exp(-(d-18)/27), & 18 < d < 37 \\ 0.5, & d \ge 37 \end{cases}$
UMi	$P_{LOS} = \min(18/d, 1) \cdot (1 - \exp(-d/36)) + \exp(-d/36)$ (for outdoor users only)
UMa	$P_{LOS} = \min(18/d, 1) \cdot (1 - \exp(-d/63)) + \exp(-d/63)$
SMa	$P_{LOS} = \begin{matrix} 1, d \le 10 \\ \exp(-(d-10)/200), d > 10 \end{matrix}$
RMa	$P_{LOS} = \begin{matrix} 1, d \le 10 \\ \exp\left(-\frac{d-10}{1000}\right), d > 10 \end{matrix}$

3. Calculate the pathloss according to the equations in Table 7.11
4. Generate the large-scale parameters: angular spread at BS, angular spread at MS, delay spread, shadowing, and Rice factor. All of those variables are modeled as lognormal, so that their logarithms are Gaussian variables, with correlation coefficients prescribed in Table 7.12. Furthermore, the correlation of parameters of different MSs connected to one BS (or equivalently, parameters for a single MS moving to different locations) are correlated. The correlation is modeled as exponentially decaying, with the $1/e$ decorrelation distance prescribed in Table 7.12. Correlations of links from one MS to different BSs are neglected.

[6] For system evaluations that are accepted by the ITU, the BS and MS parameters and distributions are prescribed in ITU [2008].

5. Generate delays of the taps, either according to a uniform distribution, or - when the delay distribution is exponential - according to

$$\tau'_n = -r_{DS}\sigma_{DS}\ln z_n \quad n = 1, \ldots, N \tag{7.65}$$

where z_n $(n = 1, \ldots, N)$ are i.i.d. random variables with uniform distribution $U(0, 1)$ The τ'_n variables are then ordered so that $\tau'_{(N)} > \tau'_{(N-1)} > \cdots > \tau'_{(1)}$. Then their minimum is subtracted from all, i.e. $\tau_n = \left(\tau'_{(n)} - \tau'_{(1)}\right)$, with $n = 1, \ldots, N$, so that $\tau_N > \cdots > \tau_1 = 0$. In the case of LOS, each of the τ_n is to be divided by a factor

$$D = 0.7705 - 0.0433K + 0.0002K^2 + 0.000017K^3 \tag{7.66}$$

where K is the Rice factor in dB, as given in Table 7.12. Note, however, that for the generation of the tap powers (see next step) the *un*scaled τ_n are to be used.

Table 7.11 Parameters for the path loss models

Scenario		**Path loss (dB)** ***Note*: f_c is given in GHz and distance in m!**	**Shadow fading std (dB)**	**Applicability range, antenna height default values**
Indoor Hotspot (InH)	LoS	$PL = 16.9\ \log_{10}(d) + 32.8 + 20\log_{10}(f_c)$	$\sigma = 3$	$3\,\text{m} < d < 100\,\text{m}$ $h_{ns} = 3 - 6\,\text{m}$ $h_{UT} = 1 - 2.5\,\text{m}$
	NLoS	$PL = 43.3\ \log_{10}(d) + 11.5 + 20\ \log_{10}(f_c)$	$\sigma = 4$	$10\,\text{m} < d < 150\,\text{m}$ $h_{ns} = 3 - 6\,\text{m}$ $h_{UT} = 1 - 2.5\,\text{m}$
Urban Micro (UMi)	LoS	$PL = 22.0\log_{10}(d) + 28.0 + 20\ \log_{10}(f_c)$ $PL = 40\log_{10}(d_1) + 7.8 - 18\ \log_{10}(h'_{\text{BS}}) - 18\log_{10}(h'_{\text{UT}}) + 2\log_{10}(f_c)$	$\sigma = 3$ $\sigma = 3$	$10\,\text{m} < d_1 < d'_{BP}$ (1) $d'_{BP} < d_1 < 5000\,\text{m}$ (1) $h_{BS} = 10\,\text{m}$ (1), $h_{UT} = 1.5\,\text{m}$ (1)
	NLoS	**Manhattan grid layout:** $PL = \min(PL(d_1, d_2), PL(d_2, d_1))$ where: $PL(d_k, d_t) = PL_{LOS}(d_k) + 17.9 - 12.5\,\text{n}_j + 10\,\text{n}_j\log_{10}(d_l) + 3\log_{10}(f_c)$ and $n_j = \max(2.8 - 0.0024d_k, 1.84)$ PL_{LOS} path loss of scenario UMi LoS and $k, l \in \{1, 2\}$. **Hexagonal cell layout:** $PL = 36.7\ \log_{10}(d) + 22.7 + 26\ \log_{10}(f_c)$	$\sigma = 4$ $\sigma = 4$	$10\,\text{m} < d_1 + d_2 < 5000\,\text{m}$, $w/2 < \min(d_1, d_2)$ (2) $w = 20\,\text{m}$ (street width) $h'_{BS} = 10\,\text{m}$, $h_{UT} = 1.5\,\text{m}$. When $0 < \min(d_1, d_2) < w/2$, the LoS PL is applied. $10\,\text{m} < d < 2000\,\text{m}$ $h_{BS} = 10\,\text{m}$ $h_{UT} = 1 - 2.5\,\text{m}$
	O-to-I	$PL = PL_b + PL_{tw} + PL_{in}$ **Manhattan grid layout (θ known):** $\begin{cases} PL_b = PL_{B1}(d_{out} + d_{iv}) \\ PL_{tw} = 14 + 15(1 - \cos(\theta))^2 \\ PL_{in} = 0.5d_{in} \end{cases}$ **For hexagonal layout(θ unknown):** $PL_{tw} = 20$, other values remain the same.	$\sigma = 7$	$10\,\text{m} < d_{out} + d_{in} < 1000\,\text{m}$, $0\,\text{m} < d_{in} < 25\,\text{m}$, $h_{BS} = 10\,\text{m}, h_{UT} = 3(n_{Fl} - 1) + 1.5\,\text{m}$, $n_{Fl} = 1$ *Explanations* : see(3)

Scenario		Path loss (dB) *Note*: f_c is given in GHz and distance in m!	Shadow fading std (dB)	Applicability range, antenna height default values
Urban Macro (UMa)	LoS	$PL = 22.0 \log_{10}(d) + 28.0 + 20 \log_{10}(f_c)$	$\sigma = 4$	$10\,\text{m} < d < d'_{BP}$ [1]
		$PL = 40.0 \log_{10}(d_1) + 7.8 - 18.0 \log_{10}(h'_{BS}) - 18.0 \log_{10}(h'_{UT}) + 2.0 \log_{10}(f_c)$	$\sigma = 4$	$d'_{BP} < d < 5000\,\text{m}$ [1] $h_{BS} = 25\,\text{m}$ [1], $h_{UT} = 1.5\,\text{m}$ [1]
	NLoS	$PL = 161.04 - 7.1 \log_{10}(W) + 7.5 \log_{10}(h) - (24.37 - 3.7(h/h_{BS})^2) \log_{10}(h_{BS}) + (43.42 - 3.1 \log_{10}(h_{BS}))(\log_{10}(d) - 3) + 20 \log_{10}(f_c) - (3.2(\log_{10}(11.75 h_{UT}))^2 - 4.97)$	$\sigma = 6$	$10\,\text{m} < d < 5\,000\,\text{m}$ h = avg. building height W = street width $h_{BS} = 25\,\text{m}$, $h_{UT} = 1.5\,\text{m}$, $W = 20\,\text{m}$, $h = 20\,\text{m}$ The applicability ranges: $5\,\text{m} < h < 50\,\text{m}$ $5\,\text{m} < W < 50\,\text{m}$ $10\,\text{m} < h_{BS} < 150\,\text{m}$ $1\,\text{m} < h_{UT} < 10\,\text{m}$
Suburban Macro (SMa, optional)	LoS	$PL_1 = 20 \log_{10}(40\pi d f_c/3) + \min(0.03h^{1.72}, 10) \log_{10}(d) - \min(0.044h^{1.72}, 14.77) + 0.002 \log_{10}(h) d$	$\sigma = 4$	$10\,\text{m} < d < d_{BP}$ [4]
		$PL_2 = PL_1(d_{BP}) + 40 \log_{10}(d/d_{BP})$	$\sigma = 6$	$d_{BP} < d < 5000\,\text{m}$ $h_{BS} = 35\,\text{m}$, $h_{UT} = 1.5\,\text{m}$, $W = 20\,\text{m}$, $h = 10\,\text{m}$ (The applicability ranges of h, W, h_{BS}, h_{UT} are same as in UMa NLoS)
	NLoS	$PL = 161.04 - 7.1 \log_{10}(W) + 7.5 \log_{10}(h) - (24.37 - 3.7(h/h_{BS})^2) \log_{10}(h_{BS}) + (43.42 - 3.1 \log_{10}(h_{BS}))(\log_{10}(d) - 3) + 20 \log_{10}(f_c) - (3.2(\log_{10}(11.75 h_{UT}))^2 - 4.97)$	$\sigma = 8$	$10\,\text{m} < d < 5000\,\text{m}$ $h_{BS} = 35\,\text{m}$, $h_{UT} = 1.5\,\text{m}$, $W = 20\,\text{m}$, $h = 10\,\text{m}$ (Applicability ranges of h, W, h_{BS}, h_{UT} are same as in UMa NLoS)
Rural Macro (RMa)	LoS	$PL_l = 20 \log_{10}(40\pi d f_c/3) + \min(0.03h^{1.72}, 10) \log_{10}(d) - \min(0.044h^{1.72}, 14.77) + 0.002 \log_{10}(h) d$	$\sigma = 4$	$10\,\text{m} < d < d_{BP}$ [4]
		$PL_2 = PL_1(d_{BP}) + 40 \log_{10}(d/d_{BP})$	$\sigma = 6$	$d_{BP} < d < 10000\,\text{m}$, $h_{BS} = 35\,\text{m}$, $h_{UT} = 1.5\,\text{m}$, $W = 20\,\text{m}$, $h = 5\,\text{m}$ (Applicability ranges of h, W, h_{BS}, h_{UT} are same as UMa NLoS)
	NLoS	$PL = 161.04 - 7.1 \log_{10}(W) + 7.5 \log_{10}(h) - (24.37 - 3.7(h/h_{BS})^2) \log_{10}(h_{BS}) + (43.42 - 3.1 \log_{10}(h_{BS}))(\log_{10}(d) - 3) + 20 \log_{10}(f_c) - (3.2(\log_{10}(11.75 h_{UT}))^2 - 4.97)$	$\sigma = 8$	$10\,\text{m} < d < 5000\,\text{m}$ $h_{BS} = 35\,\text{m}$, $h_{UT} = 1.5\,\text{m}$, $W = 20\,\text{m}$, $h = 5\,\text{m}$ (Applicability ranges of h, W, h_{BS}, h_{UT} are same as UMa NLoS)

Table 7.12 Parameters for channel model in various environments

Scenarios		IaH		UMi			SMa		UMa		RMa	
		LoS	NLoS	LoS	NLoS	O-in-I	LoS	NLoS	LoS	NLoS	LoS	NLoS
Delay spread (DS) $\log_{10}(s)$	μ	−7.70	−7.41	−7.19	−6.89	−6.62	−7.23	−7.12	−7.03	−6.44	−7.49	−7.43
	σ	0.18	0.14	0.40	0.54	0.32	0.38	0.33	0.66	0.39	0.55	0.48
AoD spread (ASD) $\log_{ns10}$ (degrees)	μ	1.60	1.62	1.20	1.41	1.25	0.78	0.90	1.15	1.41	0.90	0.95
	σ	0.18	0.25	0.43	0.17	0.42	0.12	0.36	0.28	0.28	0.38	0.45
AoA spread (ASA) $\log_{10}$ (degrees)	μ	1.62	1.77	1.75	1.84	1.76	1.48	1.65	1.81	1.87	1.52	1.52
	σ	0.22	0.16	0.19	0.15	0.16	0.20	0.25	0.20	0.11	0.24	0.13
Shadow fading (SF) (dB)	σ	3	4	3	4	7	4	8	4	6	4	8
K-factor (K) (dB)	μ	7	N/A	9	N/A	N/A	9	N/A	9	N/A	7	N/A
	σ	4	N/A	5	N/A	N/A	7	N/A	3.5	N/A	4	N/A
Cross-correlations*	ASD vs DS	0.6	0.4	0.5	0	0.4	0	0	0.4	0.4	0	−0.4
	ASA vs DS	0.8	0	0.8	0.4	0.4	0.8	0.7	0.8	0.6	0	0
	ASA vs SF	−0.5	−0.4	−0.4	−0.4	0	−0.5	0	−0.5	0	0	0
	ASD vs SF	−0.4	0	−0.5	0	0.2	−0.5	−0.4	−0.5	−0.6	0	0.6
	DS vs SF	−0.8	−0.5	−0.4	−0.7	−0.5	−0.6	−0.4	−0.4	−0.4	−0.5	−0.5
	ASD vs ASA	0.4	0	0.4	0	0	0	0	0	0.4	0	0
	ASD vs K	0	N/A	−0.2	N/A	N/A	0	N/A	0	N/A	0	N/A
	ASA vs K	0	N/A	−0.3	N/A	N/A	0	N/A	−0.2	N/A	0	N/A
	DS vs K	−0.5	N/A	−0.7	N/A	N/A	0	N/A	−0.4	N/A	0	N/A
	SF vs K	0.5	N/A	0.5	N/A	N/A	0	N/A	0	N/A	0	N/A
Delay distribution		Exp	Exp	Exp	Exp	Exp	Exp	Exp	Exp	Exp	Exp	Exp
AoD and AoA distribution		Laplacian		Wrapped Gaussian			Wrapped Gaussian		Wrapped Gaussian		Wrapped Gaussian	
Delay scaling parameter r_τ		3.6	3	3.2	3	2.2	2.4	1.5	2.5	2.3	3.8	1.7
XPR (dB)	μ	11	10	9	8.0	9	8	4	8	7	12	7
Number of clusters		15	19	12	19	12	15	14	12	20	11	10
Number of rays per cluster		20	20	20	20	20	20	20	20	20	20	20
Cluster ASD		5	5	3	10	5	5	2	5	2	2	2
Cluster ASA		8	11	17	22	8	5	10	11	15	3	3
Per cluster shadowing std ζ (dB)		6	3	3	3	4	3	3	3	3	3	3
Correlation distance (m)	DS	8	5	7	10	10	6	40	30	40	50	36
	ASD	7	3	8	10	11	15	30	18	50	25	30
	ASA	5	3	8	9	17	20	30	15	50	35	40
	SF	10	6	10	13	7	40	50	37	50	37	120
	K	4	N/A	15	N/A	N/A	10	N/A	12	N/A	40	N/A

6. Generate the average powers of the N taps as

$$P'_n = e^{\frac{(1-r_{DS})\tau_n}{r_{DS}\cdot\sigma_{DS}}} \cdot 10^{-0.1\xi_n} \qquad n = 1, \ldots, N. \tag{7.67}$$

ξ_n for $n = 1, \ldots, N$ are the cluster shadowing terms. Average powers are then normalized, so that the total average power for all N paths is equal to unity. Each ray in a tap is assigned $1/M = 1/20$ of the tap power.

7. Generate the angles of arrival. The angular spectra are modeled as wrapped Gaussians, except for the indoor hotspot scenario, where it is Laplacian. The angles are computed in the Gaussian case as

$$\theta'_n = \frac{2\sigma_{\mathrm{AOA}}\sqrt{-\ln(P_n/\max(P_n))}}{C} \tag{7.68}$$

and for the Laplacian case

$$\theta'_n = -\frac{\sigma_{\mathrm{q}}\ln(P_n/\max(P_n))}{C} \tag{7.69}$$

where $\sigma_{\mathrm{AOA}} = \sigma_{\mathrm{q}}/1.4$ is the standard deviation. The scaling constant C is a scaling factor related to the number of clusters, and is given in Table 7.13. In the case of LOS, the scaling constant has to be replaced by

$$C^{\mathrm{LOS}} = C\left(1.1035 - 0.028K - 0.002K^2 + 0.0001K^3\right) \tag{7.70}$$

$$C^{\mathrm{LOS}} = C\left(0.9275 + 0.0439K - 0.0071K^2 + 0.0002K^3\right) \tag{7.71}$$

for Gaussian and Laplacian spectrum, respectively.
The mean angles θ_n are then computed as

$$\theta_n = X_n\theta_n + Y_n + \theta_{\mathrm{LOS}} \tag{7.72}$$

where X_n is a random variable that equiprobably takes on the values $+1$ and -1, Y_n is a normally distributed random variable with standard deviation $\sigma_{\mathrm{q}}/7$, and θ_{LOS} is the arrival angle of the LOS component (which is known from gometrical considerations).

For the LOS case, θ_n is normalized by subtracting $X_1\theta_1 + Y_1$ from every θ_n; this enforces that the first cluster is seen in the direction θ_{LOS}. The angles of the rays are computed by adding the offset angles (where the angles given in Table 7.14 have to be multiplied by the cluster angular spread) to the mean angles θ_n of each cluster.

The same procedure applies for the angles of departure

8. Perform a random coupling of the ray AOAs and AODs within each tap (or subcluster, see below).
9. For each ray, and each polarization (vv, vh, hv, hh) draw an initial random phase Φ from a uniform distribution in $[-\pi, \pi]$. In the LOS case, also draw a random initial phase for the LOS component for the vv and hh polarization.
10. For the two strongest taps, split the taps into "subclusters", according to Table 7.15, so that some of the taps have a delay offset compared to the nominal computed delays. For the weaker clusters, no such splitting is done. Compute the polarized impulse responses at the antenna elements as

$$\begin{aligned} h^{\mathrm{NLOS}}_{u,s,n}(t) = \sqrt{P_n}\sum_{m=1}^{M}\Big(& e^{jk\|\mathbf{v}\|\cos(\theta_{n,m,AoA}-\theta_v)t} \\ & \mathbf{G}_{TX}(\theta_{n,m,AoD})\cdot\begin{bmatrix} \exp\left(j\Phi^{\mathrm{vv}}_{n,m}\right) & \kappa^{-1/2}\exp\left(j\Phi^{\mathrm{vh}}_{n,m}\right) \\ \kappa^{-1/2}\exp\left(j\Phi^{\mathrm{hv}}_{n,m}\right) & \exp\left(j\Phi^{\mathrm{hh}}_{n,m}\right)\end{bmatrix} \\ & \mathbf{G}_{RX}(\theta_{n,m,AoA})\cdot e^{jkd_{u,n,m}}e^{j(kd_{s,n,m})} \end{aligned} \tag{7.73}$$

Table 7.13

No. clusters	4	5	8	10	11	12	14	15	15 (InH)	16	19	19 (InH)	20
C	0.779	0.860	1.018	1.090	1.123	1.146	1.190	1.211	1.434	1.226	1.273	1.501	1.289

Table 7.14 Ray offset angles within a cluster, given for 1 degree rms angle spread

Ray number, m	Basis vector of offset angles, α_{ms}
1,2	±0.0447
3,4	±0.1413
5,6	±0.2492
7,8	±0.3715
9,10	±0.5129
11,12	±0.6797
13,14	±0.8844
15,16	±1.1481
17,18	±1.5195
19,20	±2.1551

Table 7.15 Sub-cluster information for intra cluster delay spread clusters

Sub-cluster No.	Mapping to rays	Power	Delay offset
1	1, 2, 3, 4, 5, 6, 7, 8, 19, 20	10/20	0 ns
2	9, 10, 11, 12, 17, 18	6/20	5 ns
3	13, 14, 15, 16	4/20	10 ns

where $\mathbf{G}_{TX}(\theta_{n,m,AoD})$ is a 2×1 vector containing the transmit antenna pattern for vertical and horiztonal polarization, and $d_{s,n,m}$ is the projection of the distance vector from the reference antenna element to antenna element s onto a line in the direction $\theta_{n,m,AoD}$:

$$\frac{\sqrt{x_s^2 + y_s^2}\cos\left(\arctan\left(y_s/x_s\right) - \theta_{n,m,AoA}\right)}{\sin(\theta_{n,m,AoA})} \tag{7.74}$$

in the case of a uniform linear array, this becomes $d_s \sin(\theta_{n,m,AoD})$.

In the case of LOS, add a component, so that the overall impulse response in the LOS situation is

$$\begin{aligned} h_{u,s,n}^{\mathrm{LOS}}(t) = \sqrt{\frac{1}{1+K}} h_{u,s,n}^{\mathrm{NLOS}}(t) + \delta(n-1)\sqrt{\frac{K}{1+K}} \left(e^{jk\|\mathbf{v}\|\cos(\theta_{LOS}-\theta_v)t}\right. \\ \mathbf{G}_{TX}(\theta_{n,m,LOS}) \cdot \begin{bmatrix} \exp\left(j\Phi_{\mathrm{LOS}}^{\mathrm{vv}}\right) & 0 \\ 0 & \exp\left(j\Phi_{\mathrm{LOS}}^{\mathrm{hh}}\right) \end{bmatrix} \\ \left.\mathbf{G}_{RX}(\theta_{n,m,LOS}) \cdot e^{jkd_{u,LOS}} e^{j(kd_{s,LOS})}\right. \end{aligned} \tag{7.75}$$

11. Apply the pathloss and (bulk) shadowing to the overall impulse response.

7.6.7 Appendix 7.G: The 802.15.4a UWB Channel Model

The IEEE 802.15.4a group defined ultrawideband channel models: one model for office environments below 1 GHz, one model for body-area networks, and one group of models for indoor residential, indoor office, outdoor, and industrial environments. In this appendix, we only describe the last group of models, since it is the most frequently used. The other models are discussed in Molisch et al. [2006].

We assume that the path gain as a function of the distance and frequency can be written as a product of the terms

$$G(f,d) = G(f) \cdot G(d). \tag{7.76}$$

where the frequency dependence of the channel path gain is

$$\sqrt{G(f)} \propto f^{-\kappa} \tag{7.77}$$

where κ is the frequency dependency decaying factor. The distance dependence is given by the standard power-decay law Eq. (3.8) with a breakpoint distance of 1 m, combined with lognormal shadowing (Sec. 5.8).

The power delay profile is given by a modified Saleh-Valenzuela model (Sec. 7.3.3)

$$h_{\text{discr}}(t) = \sum_{l=0}^{L} \sum_{k=0}^{K} a_{k,l} \exp(j\phi_{k,l}) \delta(t - T_l - \tau_{k,l}), \tag{7.78}$$

where the phases $\phi_{k,l}$ are uniformly distributed in [0,2π) with a number of clusters that is Poisson distributed.

$$pdf_L(L) = \frac{(\overline{L})^L \exp(-\overline{L})}{L!} \tag{7.79}$$

so that the mean $\overline{L}$ completely characterizes the distribution.

By definition, we have $\tau_{0,l} = 0$. The distributions of the cluster arrival times are given by a Poisson process

$$p(T_l | T_{l-1}) = \Lambda_l \exp\left[-\Lambda_l (T_l - T_{l-1})\right], \; l > 0 \tag{7.80}$$

where Λ_l is the cluster arrival rate (assumed to be independent of l). The classical SV model also uses a Poisson process for the ray arrival times. Due to the discrepancy in the fitting for the indoor residential, indoor office, and outdoor environments, we model ray arrival times with a mixture of two Poisson processes as

$$\begin{aligned} p\left(\tau_{k,l} | \tau_{(k-1),l}\right) &= \beta \lambda_1 \exp\left[-\lambda_1 \left(\tau_{k,l} - \tau_{(k-1),l}\right)\right] \\ &+ (1-\beta)\, \lambda_2 \exp\left[-\lambda_2 \left(\tau_{k,l} - \tau_{(k-1),l}\right)\right], \quad k > 0 \end{aligned} \tag{7.81}$$

where β is the mixture probability, while λ_1 and λ_2 are the ray arrival rates.

For some environments, most notably the industrial environment, a "dense" arrival of MPCs was observed, i.e., each resolvable delay bin contains significant energy. In that case, the concept of ray arrival rates loses its meaning, and a realization of the impulse response based on a tapped delay line model with regular tap spacings is to be used.

The next step is the determination of the cluster powers and cluster shapes. The PDP (mean power of the different paths) is exponential within each cluster

$$E\{|a_{k,l}|^2\} \propto \Omega_l \exp(-\tau_{k,l}/\gamma_l) \tag{7.82}$$

where Ω_l is the integrated energy of the l^{th} cluster, and γ_l is the intra-cluster decay time constant.

Another important deviation from the classical SV model is that we find the cluster decay time to depend on the arrival time of the cluster. In other words, the larger the delay, the larger the decay time of the cluster. A linear dependence

$$\gamma_l \propto k_\gamma T_l + \gamma_0 \tag{7.83}$$

where k_γ describes the increase of the decay constant with delay, gives good agreement with measurement values.

The energy of the l^{th} cluster, normalized to γ_l, and averaged over the cluster shadowing and the small-scale fading, follows in general an exponential decay

$$10\log(\Omega_l) = 10\log(\exp(-T_l/\Gamma)) + M_{\text{cluster}} \tag{7.84}$$

where M_{cluster} is a normally distributed variable with standard deviation σ_{cluster}.

For the non-LOS (NLOS) case of some environments (office and industrial), the above description is not a good model for the PDP. Rather, we observe only a single cluster, whose power first increases (with increasing delay), goes through a maximum, and then decreases again. Such a shape of the PDP can significantly influence the ranging and geolocation performance of UWB systems, as ranging algorithms require the identification of the first (not the strongest) MPC.

Table 7.16 Parameters for channel models CM 1 and CM 2 (residential)

Residential valid range of d	LOS 7 – 20 m	NLOS 7 – 20 m
Path gain		
G_0 [dB]	−43.9	−48.7
n	1.79	4.58
$S[dB]$	2.22	3.51
κ	1.12	1.53
Power delay profile		
$\overline{L}$	3	3.5
Λ [1/ns]	0.047	0.12
λ_1, λ_2 [1/ns], β	1.54, 0.15, 0.095	1.77, 0.15, 0.045
Γ [ns]	22.61	26.27
k_γ	0	0
γ_0 [ns]	12.53	17.50
σ_{cluster} [dB]	2.75	2.93
Small-scale fading		
m_0 [dB]	0.67	0.69
$\widehat{m}_0$ [dB]	0.28	0.32
$\widetilde{m}_0$	NA	NA

Table 7.17 Parameters for channel models CM 3 and CM 4 (office)

Office valid range of d	LOS 3 – 28 m	NLOS 3 – 28 m
Path gain		
n	1.63	3.07
σ_S	1.9	3.9
G_0 [dB]	−35.4	−59.9
κ	0.03	0.71
Power delay profile		
$\overline{L}$	5.4	1
Λ [1/ns]	0.016	NA
λ_1, λ_2 [1/ns], β	0.19, 2.97, 0.0184	NA
Γ [ns]	14.6	NA
k_γ	0	NA
γ_0 [ns]	6.4	NA
σ_{cluster} [dB]	3	NA
Small-scale fading		
m_0	0.42 dB	0.50 dB
$\widehat{m}_0$	0.31	0.25
$\widetilde{m}_0$	NA	NA
χ	NA	0.86
γ_{rise}	NA	15.21
γ_1	NA	11.84

Table 7.18 Parameters for channel models CM 5, CM 6, and CM 9 (outdoor LOS, outdoor NLOS, and farm environments)

Outdoor valid range of d	LOS 5 – 17 m	NLOS 5 – 17 m	Farm
Path gain			
n	1.76	2.5	1.58
σ_S	0.83	2	3.96
G_0	−45.6	−73.0	−48.96
κ	0.12	0.13	0
Power delay profile			
$\overline{L}$	13.6	10.5	3.31
Λ [1/ns]	0.0048	0.0243	0.0305
λ_1 [1/ns]	0.27	0.15	0.0225, 0, 0
λ_2 [1/ns]	2.41	1.13	
β	0.0078	0.062	
Γ [ns]	31.7	104.7	56
k_γ	0	0	0
γ_0 [ns]	3.7	9.3	0.92
σ_{cluster} [dB]	3	3	3
Small-scale fading			
m_0	0.77 dB	0.56 dB	4.1 dB
$\widehat{m}_0$	0.78	0.25	2.5 dB
$\widetilde{m}_0$	NA	NA	0

Table 7.19 Parameters for channel models CM 7 and CM 8 (industrial)

Industrial valid range of d	LOS 2 – 8 m	NLOS 2 – 8 m
Path gain		
n	1.2	2.15
σ_S [dB]	6	6
G_0 [dB]	−56.7	−56.7
κ	−1.103	−1.427
Power delay profile		
$\overline{L}$	4.75	1
Λ [1/ns]	0.0709	NA
λ [1/ns]	NA	NA
Γ	13.47	NA
k_γ	0.926	NA
γ_0	0.651	NA
σ_{cluster} [dB]	4.32	NA
Small-scale fading		
m_0	0.36 dB	0.30 dB
$\widehat{m}_0$	1.13	1.15
$\widetilde{m}_0$ dB	12.99	
χ	NA	1
γ_{rise} [ns]	NA	17.35
γ_1 [ns]	NA	85.36

We found in the course of our investigation that the following functional fit gives a good description:

$$E\{|a_{k,1}|^2\} \propto (1 - \chi \cdot \exp(-\tau_{k,l}/\gamma_{\text{rise}})) \cdot \exp(-\tau_{k,l}/\gamma_1). \tag{7.85}$$

Here, the parameter χ describes the attenuation of the first component, the parameter γ_{rise} determines how fast the PDP increases to its local maximum, and γ_1 determines the decay at later times. The numerical values of the parameters used in Eq. (7.76)–(7.85) are specified, for different environments, in Tables 7.16–7.19.